AGU PUBLICATIONS

Geophysical Research Letters

RESEARCH LETTER
10.1002/2017GL074722

Key Points:
- Frequency of cyclones originating from lower latitudes over the South Pacific Ocean is highly correlated with Ellsworth Land accumulation
- Six of the top 10 precipitation events coincide with cyclones from lower latitudes during the autumn and winter seasons
- There are no trends in cyclone activity over the satellite record that can explain the observed accumulation trend over Ellsworth Land

Supporting Information:
- Supporting Information S1

Correspondence to:
J. S. Hosking,
jask@bas.ac.uk

Citation:
Hosking, J. S., R. Fogt, E. R. Thomas, V. Moosavi, T. Phillips, J. Coggins, and D. Reusch (2017), Accumulation in coastal West Antarctic ice core records and the role of cyclone activity, *Geophys. Res. Lett.*, *44*, 9084–9092, doi:10.1002/2017GL074722.

Received 30 JUN 2017
Accepted 17 AUG 2017
Accepted article online 22 AUG 2017
Published online 9 SEP 2017

Accumulation in coastal West Antarctic ice core records and the role of cyclone activity

J. Scott Hosking[1], Ryan Fogt[2], Elizabeth R. Thomas[1], Vahid Moosavi[3], Tony Phillips[1], Jack Coggins[4], and David Reusch[5]

[1]British Antarctic Survey, NERC, Cambridge, UK, [2]Department of Geography, Ohio University, Athens, Ohio, USA, [3]Computer Aided Architectural Design, Institute of Technology in Architecture, Department of Architecture, ETH Zurich, Zurich, Switzerland, [4]London, UK, [5]Department of Earth and Environmental Science, New Mexico Institute of Mining and Technology, Socorro, New Mexico, USA

Abstract Cyclones are an important component of Antarctic climate variability, yet quantifying their impact on the polar environment is challenging. We assess how cyclones which pass through the Bellingshausen Sea affect accumulation over Ellsworth Land, West Antarctica, where we have two ice core records. We use self-organizing maps (SOMs), an unsupervised machine learning technique, to group cyclones into nine SOM nodes differing by their trajectories (1980–2015). The annual frequency of cyclones associated with the first SOM node (SOM1, which generally originate from lower latitudes over the South Pacific Ocean) is significantly ($p < 0.001$) correlated with annual accumulation, with the highest seasonal correlations ($p < 0.001$) found during autumn. While significant ($p < 0.01$) increases in vertically integrated water vapor over the South Pacific Ocean coincide with this same group of cyclones, we find no indication that this has led to an increase in moisture advection into, nor accumulation over, Ellsworth Land over this short time period.

Plain Language Summary Cyclones are an important component of Antarctic climate variability, yet quantifying their impact on the polar environment is challenging. We assess how cyclones which pass through the Bellingshausen Sea affect snowfall over Ellsworth Land, West Antarctica, where we have two ice core records. We use a novel machine learning technique to group cyclones differing by their pathways. The annual frequency of cyclones associated with cyclones which generally originate from lower latitudes over the South Pacific Ocean is significantly correlated with annual snowfall, with the highest seasonal correlations found during autumn. While significant increases in water vapor over the South Pacific Ocean coincide with this same group of cyclones, we find no indication that this has led to an increase in the transport of moisture into, nor accumulation over, Ellsworth Land over this short time period.

1. Introduction

Over the past 60 years West Antarctica has experienced significant changes in near-surface air temperature [*Bromwich et al.*, 2013], sea ice extent [*Holland and Kwok*, 2012], and mass balance [*McMillan et al.*, 2014]. Moreover, ice core records spanning the past 300 years taken from Ellsworth Land, West Antarctica, indicate that change over recent decades has been unprecedented with respect to the past 300 years [*Thomas et al.*, 2015].

One of the primary drivers of climate variability in this region is the Amundsen Sea Low (ASL), a quasi-stationary climatological low-pressure system located in the Pacific sector of the Southern Ocean between 170–298°E and 75–60°S [*Fogt et al.*, 2012; *Turner et al.*, 2013; *Hosking et al.*, 2013, 2016; *Raphael et al.*, 2016]. This is also one of the most intense regions of cyclone activity on Earth with on average 550 cyclones passing through the Pacific sector of the Southern Ocean every year [*Fogt et al.*, 2012]. The climatological position of the ASL indicates that the Amundsen-Bellingshausen Sea region is a favored location for cyclones to end their trajectory [*Simmonds and Keay*, 2000], thus making Ellsworth Land a highly variable region for transporting moist air and atmospheric composition (tracers) into Antarctica [*Lachlan-Cope et al.*, 2001]. The relationship between cyclones and accumulation within an ice core is difficult to assess due to many factors including the trajectory source location and meteorological conditions there, the trajectory pathway and surface forcing over the trajectory, the changing cyclone depth and radius along the trajectory, the trajectory proximity to ice core site, and the cyclone frequency and time of year. Cyclones may not be the only precipitation

source in this region; onshore advection may lead to orographic precipitation, and the presence of sea ice may influence the availability of moisture [*Thomas et al*., 2015]. However, separating these processes is beyond the scope of this paper. We focus here on the cyclones, which based on previous studies highlighted above are assumed to dominate the precipitation in this region. To this end, we will focus this study on three questions:

1. How important are cyclones in driving interannual variability in the Ellsworth Land ice core accumulation records?
2. What role do cyclone trajectory pathways play in accumulation rates over the Ellsworth Land coastal zone?
3. Has there been a shift in cyclone activity which could help explain the positive trend in accumulation in Ellsworth Land?

Answering these questions is key to understanding how changes in weather patterns drive the observed changes in Antarctic accumulation rates and may also provide some insight into how cyclones have changed in the past over the length of the ice core record.

2. Methodology

We compute cyclone trajectories using the cyclone tracking scheme as outlined by *Simmonds and Keay* [2000], which is based on *Murray and Simmonds* [1991] with enhancements discussed in *Simmonds and Murray* [1999] and *Simmonds et al*. [1999]. This cyclone tracking scheme uses the Laplacian of 6-hourly ERA-Interim reanalysis [*Dee et al*., 2011] sea level pressure to calculate the central coordinates of all time points along each cyclone track. The scheme identifies cyclone radius (degrees latitude) and depth (hPa) by searching out from the local pressure Laplacian maximum associated with each cyclone in each of 18 equally spaced angular directions to identify the envelope of points surrounding the cyclone at which the Laplacian becomes negative. The cyclone radius is calculated as the radius of the circle with the same area as this envelope of points. The cyclone depth is calculated as the difference between the central pressure of the cyclone and the weighted mean of the pressures at each point on the envelope (the weights being the inverse distance between each point on the envelope and the local pressure Laplacian maximum). Other variables are also calculated by the cyclone tracking scheme, although they are not considered within this study. As input data we use 6-hourly ERA-Interim reanalysis mean sea level pressure fields at a resolution of N80 which has been shown to be highly reliable within this sector of Antarctica [*Bracegirdle and Marshall*, 2012].

To assess the impact of cyclones on Ellsworth Land, we only select those cyclones which pass through the Bellingshausen Sea region (Figure 1) and cyclones that are well defined (a closed system) at least at one point along its track.

To answer the questions outlined in section 1, the cyclone trajectories are clustered into groups using an unsupervised machine learning image recognition technique known as self-organizing maps (SOMs), which identifies general patterns in high-dimensional input data [*Kohonen*, 1984, 2001, 2013]. The SOM map is defined here as a 3×3 matrix to ensure that we have clear separation in the trajectory patterns and to limit any overlap between meridionally and zonally traveling cyclones. Although SOMs have been used within climate science before [e.g., *Reusch et al*., 2005; *Cassano et al*., 2006; *Uotila et al*., 2007; *Reusch*, 2010], this is the first time that the technique has been used to group individual cyclone tracks. To assess cyclone tracks using SOMs, we do the following:

1. For each cyclone track we define the 6-hourly point at which the cyclone is closest to the ice core sites as "closest point." For the location of the ice core site we use the average latitude and longitude location of the two neighboring Ferrigno and Bryan Coast ice core sites (276.0°E, 74.3°S). Averaging over two neighboring ice core records in this way improves the signal-to-noise ratio. All cyclone positions subsequent to the closest point are removed for the purposes of creating the SOM (i.e., where the cyclone goes after is of less interest for the climate over Ellsworth Land). The distribution of distances at the closest points among all the cyclones assessed in this study is shown in Figure S1 in the supporting information.
2. We constrain the cyclone track data to assess complete years and by selecting those cyclones where the time at the closest point lies between 1 January 1980 and 31 December 2015 inclusive. Therefore,

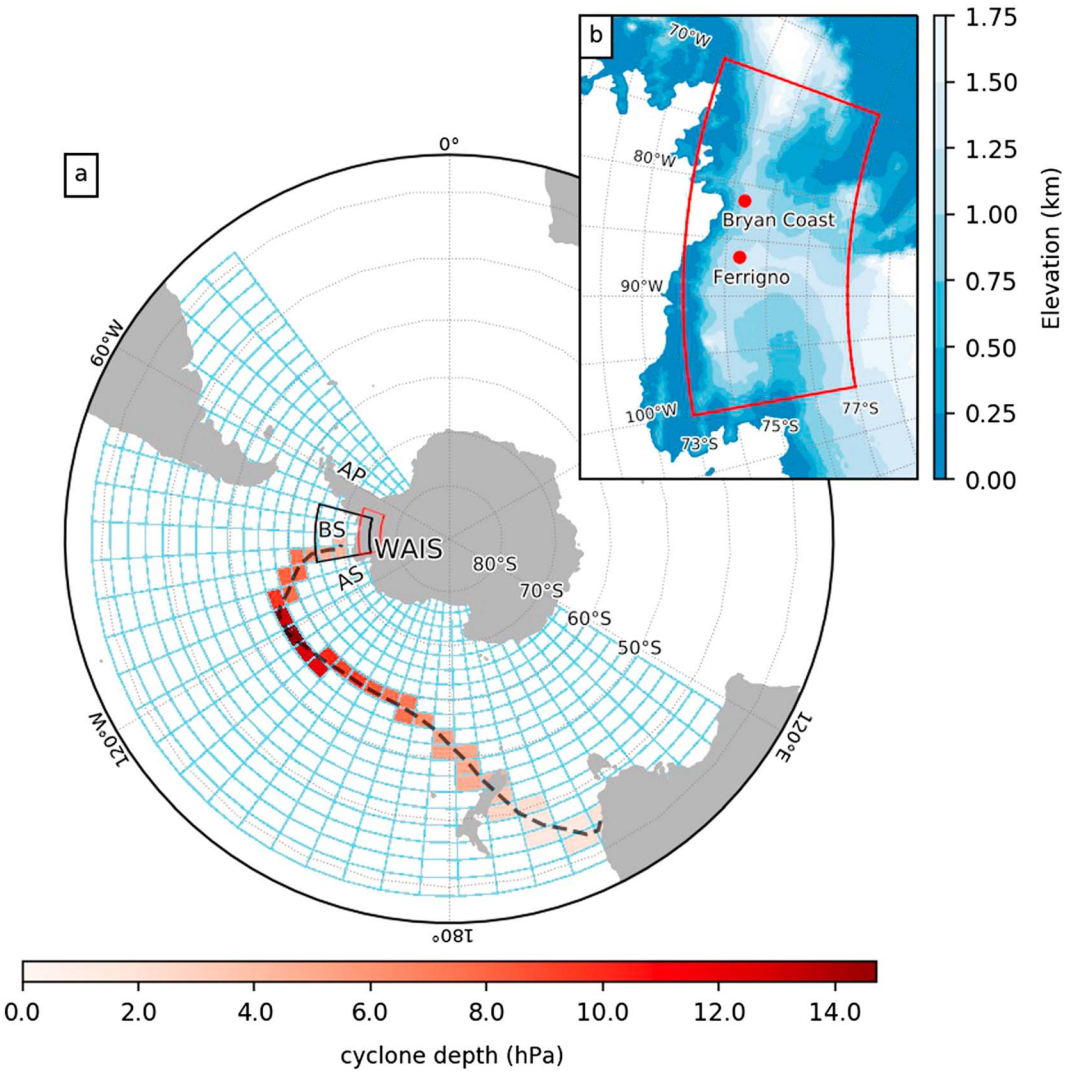

Figure 1. (a) A cyclone passing through the Bellingshausen Sea (BS, defined region shown by black solid lines), off the West Antarctic Ice Sheet (WAIS) between the Antarctic Peninsula (AP) and Amundsen Sea (AS). The cyclone pathway (black dashed line) is converted into an image on a 32 × 20 grid spanning the area 125–320°E and 30–80°S (blue grid) to represent the cyclone trajectory shape and depth along its path (white-red shading). (b) The locations of the Ferrigno and Bryan Coast ice core sites relative to the regional topography (red dots). The Ellsworth Land area in which we average accumulation is shown in Figures 1a and 1b (red line boxes).

cyclones which start within 1979 and reach the closest point in 1980 are *included*, whereas cyclones which start in 2015 but reach the closest point in 2016 are *excluded*. This ensures that we have complete cyclone trajectories from the source to the point they influence the accumulation over Ellsworth Land.

3. For each cyclone track we create a two-dimensional image which captures the shape and estimated depths of the cyclone pathways (see example in Figure 1) over the Pacific sector of the Southern Ocean (hereafter known as "images"). For this study, all images (one for each cyclone) have a specified shape of 32 × 20 grid boxes; initially, all grid points are set to zero. Then we take the 6-hourly cyclone points and linearly fit six additional points between each of the two original points. This ensures that we have a continuous set of grid points with values along the cyclone track, to fill any gaps where the cyclones moved quickly between two 6-hourly points. Then, using the estimated relative depth of the cyclone at each point, we assign the corresponding grid box that value (see red shading in Figure 1). By including the cyclone depth within these images, we are essentially reducing the influence of those sections of the cyclone pathways where the cyclone is relatively weak and shallow. Where a cyclone has two points which lie within the same grid box, we take the largest/deepest value. Thus, the shape of nonzero values within the images shows the area where cyclones have been identified. Results in this paper are relatively insensitive to the exact image grid size or number of additional points fitted between the 6-hourly points.

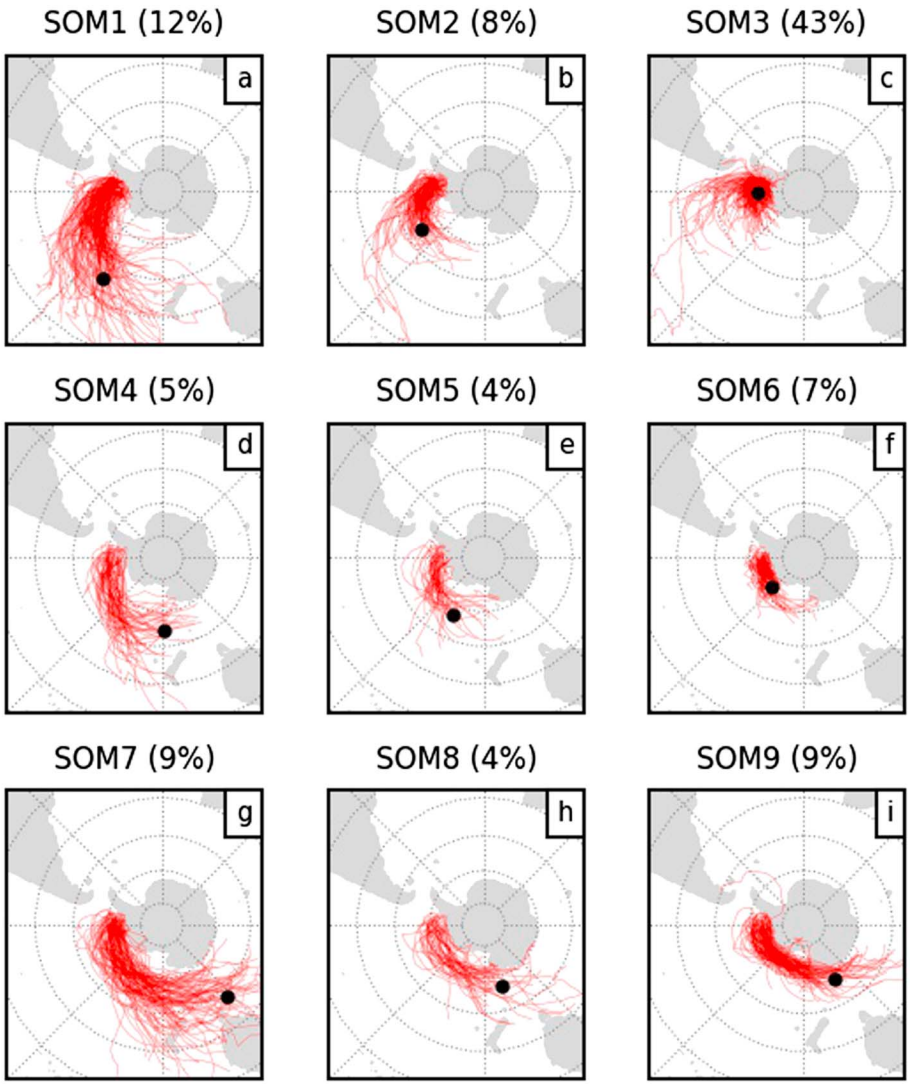

Figure 2. Nine different groups of cyclone pathways which all pass through the Bellingshausen Sea box (Figure 1). We use a 3 × 3 matrix self-organizing map (SOM) to differentiate between 5134 cyclone images. To aid visualization, we show one in every four tracks (red lines). The median cyclogenesis locations of all cyclones associated with each SOM node are shown (black dots), while the frequency of occurrence is shown as a percentage at the top of each panel.

The 5134 resulting images are clustered into nine groups, in a 3 × 3 SOM matrix using software developed by coauthor Moosavi (https://github.com/sevamoo/SOMPY) [*Moosavi*, 2017]. The cyclone tracks associated with the nine SOM nodes are shown in Figures 2a–2i.

We also use three other variables from ERA-Interim to evaluate the impact of cyclones on accumulation; these are 6-hour-averaged precipitation and evaporation rates (the difference provides the accumulation rate) and monthly vertically integrated water vapor. ERA-interim was found to capture both annual and subseasonal snow accumulation variability over the region [*Thomas and Bracegirdle*, 2015]. Lastly, we compare yearly cyclone statistics against annual composite accumulation from the Ferrigno and Bryan Coast ice core records. These records are derived using the summer maxima in non-sea-salt sulfate as described in *Thomas et al*. [2015].

3. Results

In this section, we address the three questions posed within section 1. Figure 2 illustrates the track pathways for the nine SOM nodes computed using the 5134 cyclones which pass through the Bellingshausen Sea box (Figure 1). The SOM nodes clearly differ from those that travel north to south (e.g., SOM1 and SOM2,

Figures 2a and 2b) and west to east (e.g., SOM7 and SOM9, Figures 2g and 2i) and those that lie between (e.g., SOM4 and SOM5, Figures 2d and 2e). The corresponding frequency of cyclones (relative to the total number of cyclones) associated with each SOM node is included at the top of each panel. The median latitude and longitude genesis locations for all cyclones associated with each SOM node are marked with a black dot, e.g., highlighting that the transport of SOM1 cyclones is generally meridional (north to south) thus originating from warmer latitudes and regions with higher vapor pressures, while by contrast SOM9 is zonal (west to east) where average temperatures and humidity will be lower.

3.1. How Important Are Cyclones in Driving Interannual Variability in the Ellsworth Land Ice Core Accumulation Records?

Annual time series of cyclone statistics for each SOM node are produced, namely, cyclone frequency with respect to the total number of cyclones (per year), mean radius, mean depth, and mean distance from the ice core sites (Figure S2). The three mean values (radius, depth, and distance) are calculated across all cyclone trajectories at the point closest to the ice core sites ("closest point"). While SOM3 has the greatest frequency (Figure 2), and therefore has the greatest contribution to the total overall accumulation at the ice core site, it does not explain the interannual variability within the accumulation record. Using Pearson's correlation coefficient over the overlap period (1980–2010), it was found that the annual cyclone frequency associated with SOM1 is the only time series which is significantly correlated ($r = 0.71$, $p < 0.001$) with the annual accumulation record. On subannual timescales, autumn (March, April, May (MAM)) is the only season where the seasonal frequency of SOM1 cyclones is significantly correlated ($r = 0.58$, $p < 0.001$) with the annual ice core record (see Figure S3). Thus, a greater frequency of cyclones with a more meridional/poleward, rather than zonal, trajectory pathway generally leads to higher accumulation over Ellsworth Land above the mean accumulation, which contributes to the interannual variability and drives the significant correlation during the period of overlap in Figure S3. In addition, we can see that there is no obvious relationship between cyclone activity and large El Niño events (Figure S3).

Hereafter, we mainly focus our attention on the five most frequent SOM nodes: SOM1, SOM2, SOM3, SOM7, and SOM9. These account for an average of around 17, 11, 61, 13, and 13 cyclones per year, respectively. Cyclones associated with the other four SOM nodes have frequencies less than 6% (less than nine cyclones per year).

3.2. What Role Do Cyclone Trajectory Pathways Play in Accumulation Rates Over the Ellsworth Land Coastal Zone?

In Figure 3 we assess how the timing of cyclones reaching the Bellingshausen Sea (closest point) for the SOM nodes coincides with accumulation. We do this by calculating accumulation from 6-hourly mean ERA-Interim precipitation and evaporation (which includes sublimation) spatially averaged over Ellsworth Land (260–290°E, 77–73°S; see area in Figure 1). To ensure that we capture the signal of accumulation associated with a passing cyclone, for each cyclone we sum up the accumulation over a 4 day period, centered at the time when the cyclone is at its closest point to the ice core sites (i.e., 48 h before and 48 h after). As more than one cyclone may pass through the Bellingshausen Sea around the same time it is difficult to attribute an accumulation event to any one cyclone; therefore, this analysis can only provide a qualitative indication of how cyclones associated with the different SOM nodes contribute to accumulation found over Ellsworth Land. Using box-whisker plots, we assess how the distributions of these accumulation events change with respect to how close the cyclones get to the ice core site (Figures 3a–3e). The number on top of each column shows the average number of cyclones per year associated with each box-whisker.

As shown in the top row (Figures 3a–3e), as one might expect, cyclones that come closer to the ice core site coincide with higher levels of accumulation compared to those farther away. This is true for all SOM nodes and especially for cyclones within 600 km of the ice core composite location. For cyclones associated with SOM1 and SOM2, cyclones that reach within 300 km of the ice core site (i.e., around the 20th percentile in Figure S1) coincide with a total accumulation median value of ~14 mm, while the median of all other cyclones is around half this, ~7 mm (shown by the black dotted line for comparison). In addition, large accumulation events associated with such cyclones (<300 km) are far more likely to arise from SOM1 cyclones as illustrated by the 95th percentile whisker extending to higher values (~33 mm) compared to the other SOM nodes, while SOM1 also contributes more to the interannual accumulation variability as discussed previously. Of

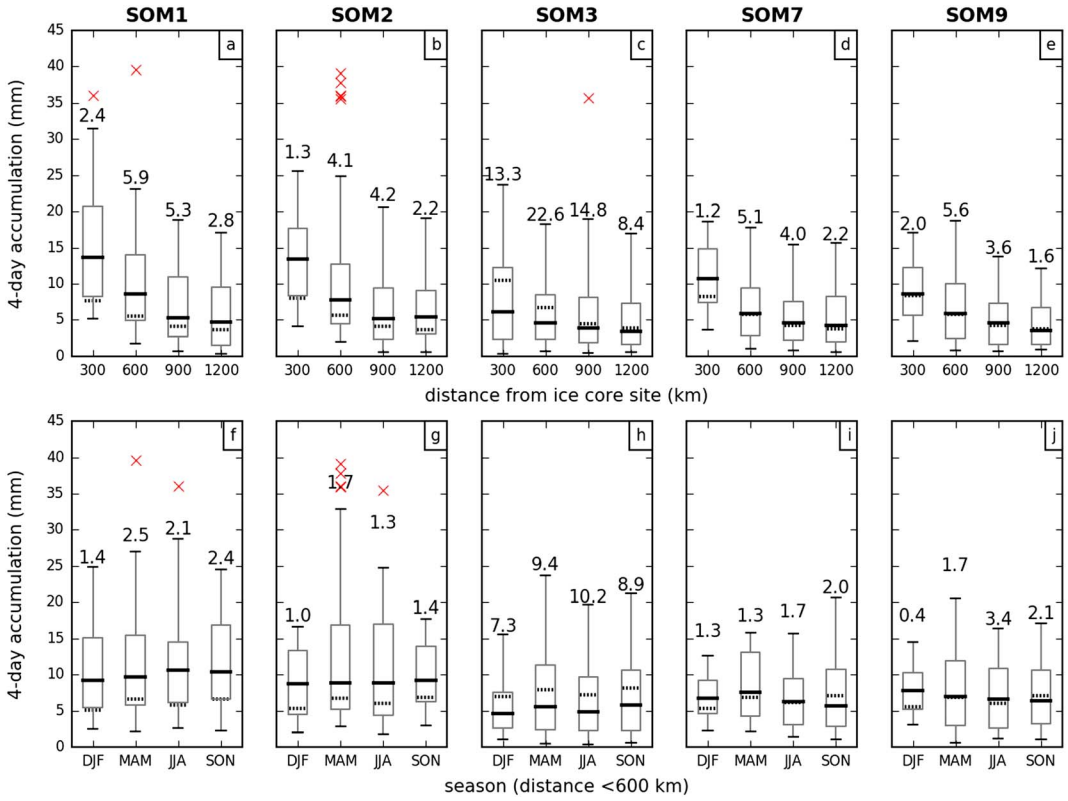

Figure 3. ERA-Interim-derived accumulation averaged over Ellsworth Land over 4 days centered over the time when cyclones are at their closest point to the composite ice core location (Figure 1). In these box-whisker plots, accumulation events are grouped into bins. These are the following: (i) distribution of events at the time the cyclone is at its closest point to the (a–e) ice core site (*x* axis labels correspond to the upper bound, e.g., 300 to 600 km is labeled as "600 km") and (ii) by season for cyclones which reach within 600 km of the (f–j) ice core location. We show the median accumulation (black thick line), the interquartile range (boxes), and the distribution range between 5% and 95% (whiskers). The median values for all other cyclones associated with other SOM nodes are shown (black dotted lines). The average corresponding number of cyclones per year is included atop each box-whisker. The 10 highest accumulation events for all cyclones are also plotted (red cross marks).

the 10 largest accumulation events over the entire record (see red "cross" markers), 6 of them are associated with SOM1 and SOM2 (north to south) cyclones and pass within 600 km of the ice core site.

Similarly, in the bottom row (Figures 3f–3j), we show the distribution of 4 day accumulation events by season for those cyclones that reach within 600 km of the ice core site (around the 55th percentile, Figure S1), where the accumulation distributions are most sensitive to the associated SOM nodes (as shown in Figures 3a–3e). Across all the SOM nodes, summer (December, January, February (DJF)) accumulation has the smallest median value, which is consistent with the precipitation climatology for the area (annual (1.7 mm/d); DJF (1.2); June, July, August (JJA) (1.8); MAM (1.9); and September, October, November (SON) (1.8)), calculated from ERA-Interim and observed from in situ weather station observations from this site [*Thomas and Bracegirdle*, 2015]. For all seasons, we see that the median values are higher in SOM1 and SOM2 (black solid line) compared to all other cyclones (black dashed line) and with the 95th percentile reaching higher compared to the zonally traveling cyclones (SOM7 and SOM9). During MAM, SOM1 and SOM2 cyclones are more likely to be associated with extreme accumulation events, with 4 of the top 10 accumulation events found in MAM (red crosses); this is again consistent with the seasonal relationship between accumulation and cyclone frequency discussed previously. During JJA, 1 of the top 10 extreme accumulation events is found in SOM1 and another in SOM2.

3.3. Has There Been a Shift in Cyclone Activity Which Could Help Explain the Positive Trend in Accumulation in Ellsworth Land?

From the yearly cyclone statistics we do not find any significant trends spanning the periods 1980 and 2015 (Figure S2) or any decadal shifts in the SOM node pathways (Figure S4). Following the findings of section 3.2

Figure 4. Trend in ERA-Interim vertically integrated water vapor over the period 1980–2015 (shading) relative to the SOM node cyclone pathways (labeled above each column). Significance ($p < 0.01$) is illustrated by cross hatching. Rows represent the seasonal time window in which cyclones reach the point closest to the ice core site: All cyclones for specified (a–e) SOM node (ALL), (f–j) summer (DJF), (k–o) autumn (MAM), (p–t) winter (JJA), and (u–y) spring (SON). The spatial difference in track pathways associated with each SOM node is illustrated by the distribution (±1 standard deviation) from the median pathway (black lines). The median cyclogenesis location is illustrated (black dot).

and Figure 3, we further examine how these cyclone statistics change when we assess only those that reach to within 600 km of the ice core site (Figure S5). As before, there is a significant ($p < 0.01$) correlation between ice core accumulation and the annual frequency in SOM1. However, we now see significant ($p < 0.01$) positive trends in the radius of SOM1 cyclones (i.e., the cyclones are becoming larger spatially) and cyclone frequency of SOM7.

To assess changes over the Southern Ocean which may impact moisture advection into Ellsworth Land, we analyze trends in vertically integrated water vapor and compare with areas cyclones travel for each SOM node (Figure 4). It is apparent that only SOM1 cyclones pass through a large area of significant ($p < 0.01$) annual increase in water vapor above the South Pacific Ocean (i.e., cyclones across all seasons, labelled "ALL"), as a result of significant increases during MAM and SON. While it may be expected that this would enhance moisture advection toward Ellsworth Land, we find no significant trends when we composite the water vapor fields at the specific times when cyclones are closest to the ice core site (Figure S6). Therefore, there is no indication that cyclones are responsible for the increases in accumulation observed over the short time period (1980–2015).

4. Discussion and Conclusions

In this study, we assess the impact that cyclones from remote locations have on the accumulation of snow over the coastal region of Ellsworth Land, Antarctica, of which we have long-term (~300 years) annual records from two ice cores. Using a technique known as self-organizing maps (SOMs), these cyclones are categorized into nine groups based on their trajectory shape (in longitude-latitude space) and the cyclone depth along the trajectories. This enables us to distinguish between meridionally traveling cyclones from warmer latitudes (SOM1 and SOM2) and zonally traveling cyclones from colder regions (SOM7 and SOM9). Other SOM nodes help to distinguish the cyclone trajectories by limiting any overlap in these two patterns.

Using this method, we find that the frequency of meridionally traveling cyclones (SOM1 and SOM2) and zonally traveling cyclones (SOM7 and SOM9) each account for around a fifth of the total number of cyclones (20% and 18%, respectively) in the Bellingshausen Sea region. Furthermore, a highly significant correlation ($p < 0.001$) between the number of cyclones associated with the meridionally traveling cyclones (SOM1) per year and the annual accumulation rate is found within the ice cores (here we use a composite of two records to reduce noise, named Bryan Coast and Ferrigno, Figure 1b). The frequency of SOM1 cyclones which reach the Bellingshausen Sea during season MAM has the highest seasonal correlation ($p < 0.001$) with the same ice core record. This indicates that the number of cyclones, and particularly those traveling meridionally from warmer latitudes, is key for driving the observed year-to-year variability in accumulation over Ellsworth Land (as evident in Figure S7).

Cyclones which reach to within 600 km of the ice core sites (around 50% of all cyclones, Figure S1) generally lead to higher values in total accumulation. The median accumulation is also higher for SOM1 and SOM2 (north to south) cyclones as they bring in more moisture from warmer latitudes (Figure S7), making them more likely to cause abrupt increases in accumulation. We illustrate this by assessing the 10 highest accumulation events over the entire record and find that 6 of these were associated with meridionally traveling cyclones in SOM1 and SOM2, 4 of which occurred during MAM.

While we show that SOM1 and SOM2 cyclone frequency is important for the year-to-year variability in accumulation over Ellsworth Land (Figures 3 and S7), it is less clear whether trends in the cyclone statistics measured (distance, radius, and depth) could help explain the observed upward trend in accumulation. This is mainly due to how sensitive the trends appear to be with respect to the range of cyclones sampled, i.e., as highlighted by reducing our sample to only those that reach to within 600 km of the ice core site (Figure S2 and S5). Moreover, while there has been a significant increase ($p < 0.01$) in vertically integrated water vapor over the southern part of the Pacific Ocean coinciding with the pathway of SOM1 cyclones, we found no indication that these cyclones were responsible for increasing moisture advection toward Ellsworth Land to explain the observed increases in accumulation observed within the ice core records.

Acknowledgments
This work was undertaken as part of the Polar Science for Planet Earth Programme of the British Antarctic Survey, Natural Environment Research Council. The ERA-Interim data are available from ECMWF (http://apps.ecmwf.int/datasets/data/interim-full-daily), while the ice core data are available from the World Data Center for Paleoclimatology (www.ncdc.noaa.gov).

References

Bracegirdle, T. J., and G. J. Marshall (2012), The reliability of Antarctic tropospheric pressure and temperature in the latest global reanalyses, *J. Clim.*, *25*, 7138–7146, doi:10.1175/JCLI-D-11-00685.1.

Bromwich, D. H., J. P. Nicolas, A. J. Monaghan, M. A. Lazzara, L. M. Keller, G. A. Weidner, and A. B. Wilson (2013), Central West Antarctica among the most rapidly warming regions on Earth, *Nat. Geosci.*, *6*(2), 139–145.

Cassano, J. J., P. Uotila, and A. Lynch (2006), Changes in synoptic weather patterns in the polar regions in the twentieth and twenty-first centuries, part 1: Arctic, *Int. J. Climatol.*, *26*, 1027–1049, doi:10.1002/joc.1306.

Dee, D. P., et al. (2011), The ERA-interim reanalysis: Configuration and performance of the data assimilation system, *Q. J. R. Meteorol. Soc.*, *137*, 553–597, doi:10.1002/qj.828.

Fogt, R. L., A. J. Wovrosh, R. A. Langen, and I. Simmonds (2012), The characteristic variability and connection to the underlying synoptic activity of the Amundsen-Bellingshausen Seas low, *J. Geophys. Res.*, *117*, D07111, doi:10.1029/2011JD017337.
Holland, P. R., and R. Kwok (2012), Wind-driven trends in Antarctic sea-ice drift, *Nat. Geosci.*, *5*(12), 872–875, doi:10.1038/ngeo1627 McMillan et al., 2014.
Hosking, J. S., A. Orr, G. J. Marshall, J. Turner, and T. Phillips (2013), The influence of the Amundsen-Bellingshausen Seas low on the climate of West Antarctica and its representation in coupled climate model simulations, *J. Clim.*, *26*, 6633–6648, doi:10.1175/JCLI-D-12-00813.1.
Hosking, J. S., A. Orr, T. J. Bracegirdle, and J. Turner (2016), Future circulation changes off West Antarctica: Sensitivity of the Amundsen Sea low to projected anthropogenic forcing, *Geophys. Res. Lett.*, *43*, 367–376, doi:10.1002/2015GL067143.
Kohonen, T. (1984), *Self-Organization and Associative Memory, Series in Information Sciences*, vol. 8, Springer, Heidelberg.
Kohonen, T. (2001), *Self-Organizing Maps*, vol. 30, Springer, Berlin. [Available at http://www.springer.com/gb/book/9783540679219.]
Kohonen, T. (2013), Essentials of the self-organizing map, *Neural Netw.*, *37*, 52–65.
Lachlan-Cope, T. A. W., M. Connolley, and J. Turner (2001), The role of the non-axisymmetric Antarctic orography in forcing the observed pattern of variability of the Antarctic climate, *Geophys. Res. Lett.*, *28*(21), 4111–4114, doi:10.1029/2001GL013465 Raphael et al., 2016.
McMillan, M., A. Shepherd, A. Sundal, K. Briggs, A. Muir, A. Ridout, A. Hogg, and D. Wingham (2014), Increased ice losses from Antarctica detected by CryoSat-2, *Geophys. Res. Lett.*, *41*, 3899–3905, doi:10.1002/2014GL060111.
Moosavi, V. (2017), Contextual mapping: Visualization of high-dimensional spatial patterns in a single geo-map computers, *Environ Urban Syst.*, *61*(2017), 1–12.
Murray, R. J., and I. Simmonds (1991), A numerical scheme for tracking cyclone centres from digital data. Part I: Development and operation of the scheme, *Aust. Meteor. Mag.*, *39*, 155–166.
Raphael, M. N., G. J. Marshall, J. Turner, R. L. Fogt, D. Schneider, D. A. Dixon, J. S. Hosking, J. M. Jones, and W. R. Hobbs (2016), The Amundsen Sea Low: Variability, Change, and Impact on Antarctic Climate, *Bull. Am. Meteorol. Soc.*, *97*(1), 111–121.
Reusch, D. B. (2010), Nonlinear climatology and paleoclimatology: Capturing patterns of variability and change with self-organizing maps, *Phys. Chem. Earth, Parts A/B/C*, *35*, 329–340.
Reusch, D. B., B. C. Hewitson, and R. B. Alley (2005), Towards ice core-based synoptic reconstructions of West Antarctic climate with artificial neural networks, *Int. J. Climatol.*, *25*, 581–610.
Simmonds, I., and K. Keay (2000), Mean Southern Hemisphere extratropical cyclone behavior in the 40-year NCEP–NCAR reanalysis, *J. Clim.*, *13*, 873–885, doi:10.1175/1520-0442(2000)013<0873:MSHECB>2.0.CO;2.
Simmonds, I., and R. J. Murray (1999), Southern extratropical cyclone behaviour in ECMWF analyses during the FROST special observing periods, *Wea. Forecasting*, *14*, 878–891.
Simmonds, I., R. J. Murray, and R. M. Leighton (1999), *A Refinement of Cyclone Tracking Methods With Data From FROST*, pp. 35–49, Aust. Meteor. Mag, Special Issue.
Thomas, E. R., and T. J. Bracegirdle (2015), Precipitation pathways for five new ice core sites in Ellsworth land, West Antarctica, *Clim. Dyn.*, *44*, 2067–2078, doi:10.1007/s00382-014-2213-6.
Thomas, E. R., J. S. Hosking, R. R. Tuckwell, R. A. Warren, and E. C. Ludlow (2015), Twentieth century increase in snowfall in coastal West Antarctica, *Geophys. Res. Lett.*, *42*, 9387–9393, doi:10.1002/2015GL065750.
Turner, J., T. Phillips, J. S. Hosking, G. J. Marshall, and A. Orr (2013), The Amundsen Sea low, *Int. J. Climatol.*, *33*(7), 1818–1829, doi:10.1002/joc.3558.
Uotila, P., A. H. Lynch, J. J. Cassano, and R. I. Cullather (2007), Changes in Antarctic net precipitation in the 21st century based on intergovernmental panel on climate change (IPCC) model scenarios, *J. Geophys. Res.*, *112*, D10107, doi:10.1029/2006JD007482.